SSRG International Journal of Electronics and Communication Engineering
ISSN: 2348-8549/ https://doi.org/10.14445/23488549/IJECE-V12I11P114

Volume 12 Issue 11, 166-172, November 2025

Original Article

Unit Cell Design Strategies and Reflection Phase Analysis for Enhanced Reflectarray Antenna Development

Prapti R. Pandya[1], M. Saradadevi[2], Namrata V. Langhnoja[3]

[1]*Department of Electronics and Communication, Government Engineering College, Rajkot, Gujarat Technological University, Ahmedabad, Gujarat, India.*
[2]*Department of Electronics and Communication, Ahmedabad Institute of Technology, Gujarat Technological University, Ahmedabad, Gujarat, India.*
[3]*Department of Electronics and Communication, L.D. College of Engineering and Technology, Gujarat Technological University, Ahmedabad, Gujarat, India.*

[1]*Corresponding Author : prpandya.4@gmail.com*

Received: 14 September 2025 Revised: 16 October 2025 Accepted: 15 November 2025 Published: 29 November 2025

Abstract *- Reflectarray Antennas exhibit low profile, ease of fabrication, and electrically steered beams, and therefore are practical alternatives to traditional parabolic reflectors and phased arrays. The performance of reflectarrays is determined by the phase response of the unit cells, which must form the appropriate distribution of phase shifts. This paper considers the design and characterization of the reflection phase of unit cells that operate in the 12–14 GHz band. Full-wave electromagnetic simulations were used to evaluate a range of configurations, including rectangular, circular, slotted patch configurations, and a swastik patch with lines extended in the same direction per slot, with the goal of attaining smooth phase variation, bandwidth, and radiation efficiency. The design methodology uses geometric parameters combined with the choice of substrate material and dimensional details to minimize angle-based phase distortion and improve operational stability ultimately. From the various geometries evaluated, the swastik-shaped patch demonstrated the best performance, approaching considerable phase shift curves. A prototype of the design was fabricated from an affordable, low-loss substrate, and experimental validation demonstrated good matching of measured to simulated performance and phase response. The work presented a workable design framework for harnessing high-performance reflectarray antennas for systems in satellite communication, radar applications, and next-generation systems in 5G. The addition of optimized unit cell designs can be effectively leveraged between applications requiring controlled phase shifting and progressive adaptation for the next antenna technology. Robust antenna designs promote wireless connectivity as well as enhanced satellite technology performances.*

Keywords *- Bandwidth, Ku-band, Polarization Stability, Reflectarray Antenna, Reflection Phase, Unit Cell Design.*

1. Introduction

Reflectarray antennas have emerged as a promising alternative to conventional parabolic reflectors and phased arrays, offering high gain, low-profile designs and electronic beam steering [1]. Unlike mechanically adjusted parabolic surfaces, reflectarrays utilize planar arrays of unit cells to control the phase of reflected waves, thereby enabling the precise formation of radiation patterns [2]. They are especially suited to the needs of contemporary wireless communication and radar, with their thin form, ease of manufacture, and compatibility with PCBs.

Increases in engineered unit cell technology since its introduction in the 1960s have made it possible to achieve broader range reflection phases with small phase errors [3]. Unit cells, typically microstrip patches, rings, or slot-based structures, are used as phase shifters, and geometry and materials are chosen to maximize bandwidth, polarization control, and reconfigurability [4]. One of the design challenges is the need for a wide, linear phase span to accurately shape the beam [5]. Multi-resonant structures, high-impedance surfaces, and metamaterial-inspired elements [6], as well as tunable designs based on varactors, MEMS, and liquid crystals, are some of the solutions [7]. The need for small-size and high-gain antennas in high-data-rate communications, satellite systems, and 5G networks has spurred the development of reflectarrays, particularly at mm-wave frequencies [8]. Such antennas are also useful in radar systems where steering precision of the beam and low RCS are essential [9-14].

This paper focuses on novel approaches to unit cell design that achieve a 360-degree phase range, increased bandwidth, and polarization stability. It investigates the role of geometry, substrate characteristics, and tuning mechanisms. It is both simulated and experimentally verified to apply to high-gain, reconfigurable, and broadband reflectarray applications in wireless and radar systems.

2. Materials and Methods

2.1. Role of the Unit Cell

The basic building block of a reflectarray antenna is the unit cell, which determines the phase of the reflection of incident electromagnetic waves to accomplish beam shaping and the intended radiation pattern. Unlike traditional parabolic reflectors, which generate phase delays through a curved surface, reflectarrays use a planar array of unit cells. This makes their performance highly dependent on geometry, material properties, and placement. An optimized cell should deliver a phase variation close to 360°, minimal reflection losses, stability under varying conditions, and high efficiency across the 12–14 GHz Ku-band.

2.2. Design and Simulation

The study began with the generation of concepts that drew inspiration from various geometries, including the square patch, concentric ring, slot-loaded designs, and a swastik-shaped patch with long lines (see Figure 1). Each geometry was modeled in ANSYS HFSS with periodic boundary conditions and Floquet ports to simulate the parameters of an infinite array environment. Reflection magnitude and phase data were derived from the base Floquet mode, enabling the accurate characterization of the metamaterial while also controlling simulation time through full-scale array simulation. Additionally, the boundaries between enslaver and enslaved persons were optimized to provide phase continuity across the opposing faces between models, and the periodicity of the unit cell was subsequently maintained at $\leq \lambda/2$ at the center frequency to help suppress higher-order modes.

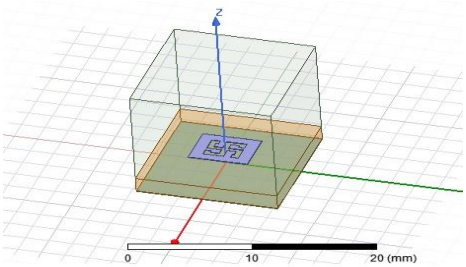

Fig. 1 Unit cell in infinite array environment

2.3. Parametric Optimization

A detailed parametric study was conducted by altering patch length and width, slot geometry, substrate thickness, and dielectric constant to achieve a phase range of greater than 330°, a smooth and monotonic phase response, a stable bandwidth across frequency and incident angle, and a reflection amplitude fluctuation of less than 1 dB. FR4 was selected as the fabrication material for its moderate dielectric constant ($\varepsilon r \approx 4.4$) and ease of availability.

2.4. Parametric Optimization

Various unit cell geometries, including rectangular, circular, slotted (with two and four slots), and swastika patches with extending lines, were examined for their reflection phase range, bandwidth, polarization stability, and fabrication feasibility. Although easy to realize, the rectangular patch has a limited phase range, which makes it less desirable in applications that require a wide range of beam steering. The circular patch has better polarization stability and symmetry, but it has a larger footprint, which restricts its use in tight designs. The slotted patches (two-slot and four-slot) have higher bandwidth and phase-tuning efficiency, but are more complex to manufacture, resulting in lower efficiency in mass production. Conversely, the swastik-shaped patch with long lines exhibited the overall best performance with compact size, high polarization stability, and could provide a 360 phase shift. Its high bandwidth, return loss, and phase control make it the best candidate for development. The geometry is also well balanced in terms of performance and complexity of design, a fact that makes it very suitable in high-frequency applications such as satellite communication and radar systems.

2.5. Prototype Integration

Following validation, the swastik unit cell design was integrated into a reflectarray prototype. Performance evaluation included beam steering capability, main lobe gain, side lobe levels, and radiation patterns across the operational 12–14 GHz bandwidth (Figure 2).

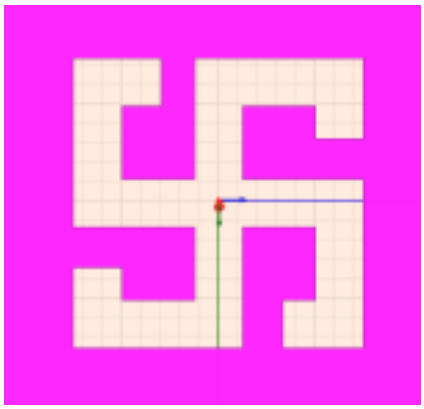

Fig. 2 Radiating element

2.6. Fabrication and Measurement

The optimized designs were fabricated on low-loss substrates using PCB techniques. Prototypes were tested in waveguide and anechoic chamber setups with a Vector Network Analyzer (VNA) calibrated using a metallic

reference. The measurements closely corresponded with the simulation results. A prototype unit cell with the swastik patch and the extended lines was created with an SMA connector for measurement (Table 1). The small scale of the unit cell was clearly demonstrated in Figure 3 by placing the unit cell in close proximity to a coin, indicating the unit cells are potentially appropriate for dense array structures.

Table 1. Dimensions of the patch

Parameters	Description	Value
Length	Patch	7.5 mm
Width	Patch	6 mm
Length	Structure	4.5 mm
Width	Structure	0.7 mm

3. Results and Discussion

3.1. Performance Comparison of Patch Geometries

Five patch geometries, mainly rectangular, circular, two-slot rectangular, four-slot rectangular, and Swastik with extended lines, were simulated for the 12–14 GHz Ku-band as shown in Table 2.

Figure 4 shows that the Swastik with extended lines achieved the best performance, offering a bandwidth of 1.67 GHz and dual resonances with deep return loss values of –26.69 dB and –33.86 dB at 13.8 GHz and 14.8 GHz, respectively. Its extended arms create alternate resonant paths, increasing electrical path length, enabling wider phase tuning, and maintaining fabrication simplicity with a single-layer structure.

Table 2. Performance comparison of patch geometries

Sr. No.	Shape	Bandwidth (GHz)	Return Loss (dB)	Centre Frequency (GHz)
1	Rectangular	1.22	–27.07	12.7
2	Circular	1.22	–26.90	12.75
3	Two slots	1.23	–17.68	13.35
4	Four slots	1.50	–22.56	13.20
5	Swastik with extended lines	1.67	–26.69, –33.86	13.8, 14.8

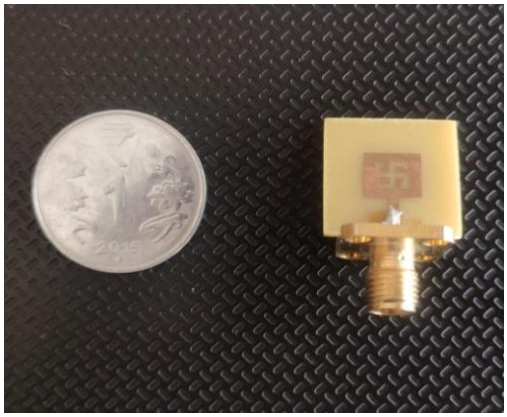

Fig. 3 Fabricated swastik-shaped unit cell with extended lines (Right) shown beside an indian 1-Rupee coin (Left) for size comparison

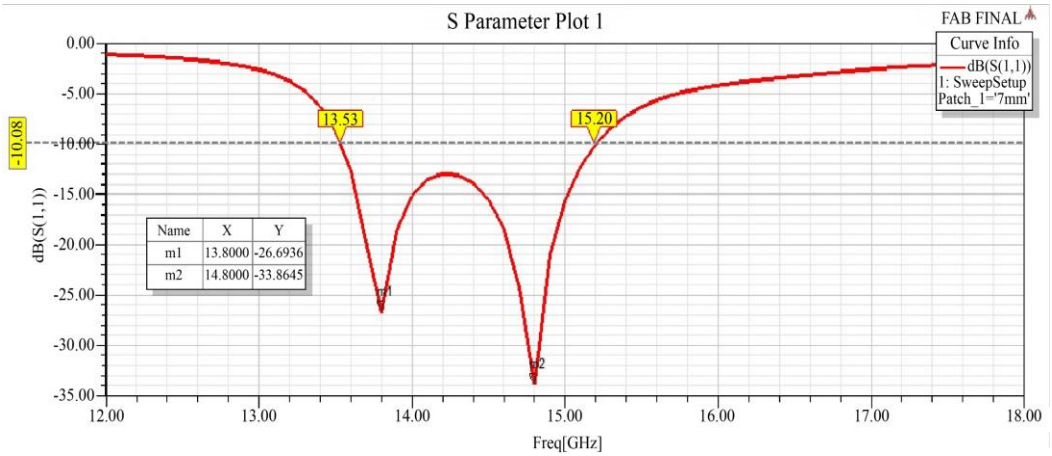

Fig. 4 Simulated S-parameter (Return Loss) of swastik patch with extended lines, showing dual resonances at 13.8 GHz and 14.8 GHz

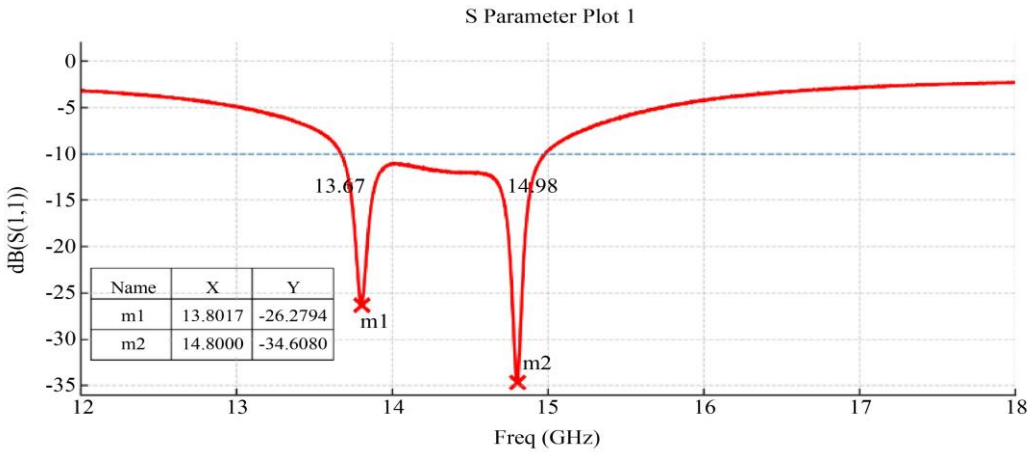

Fig. 5 Measured S-parameter of swastik patch with extended lines; The measured response closely tracks simulation with slight resonance shifts and minor bandwidth broadening

Figures 4 and 5 show close agreement between simulated and measured over the 12–14 GHz band. Small frequency shifts (tens of MHz) are consistent with PCB fabrication tolerances and modest εr/tanδ deviations; differences of a few dB in null depths reflect conductor/connector losses and SMA launch parasitics. The measured -10 dB bandwidth is marginally wider than the simulation, confirming robust dual-resonance behavior and supporting the selected unit-cell geometry.

3.2. Measurement Validation

Experimental measurements of the Swastik design confirmed the simulation results, with the measured bandwidth slightly exceeding simulated values. Variations can be attributed to fabrication tolerances, fringing field effects, soldering imperfections, or minor differences in substrate dielectric properties. In some cases, these factors enhanced radiation efficiency compared to simulations.

The reflection-phase S-curve reflects directly the manner in which the geometry of a unit cell determines its effective electrical length and thereby the phase added to an incident wave. With a fixed substrate and periodicity, the patch size or the number of current paths (e.g., slots, longer lines) will increase the length of surface current paths, shifting resonances and rotating the phase. Close-spaced, parallel S-curves across frequency are indicators of phase stability, thus greater usable bandwidth. Therefore, maximization of the Swastik geometry with longer lines aims at a wide, monotonic S-curve and large reflection strength in meeting the beam-forming conditions of 12-14 GHz.

3.3. Theoretical Basis for Reflection Phase Design

For the proposed unit element design, the variable-patch size method was employed to control the reflection phase response. By varying patch size from 2.5 mm to 5.25 mm, the design achieved a maximum reflection phase range of 278.5°. Once the 'S' curve is obtained, the reflection phase required for each element to compensate for the spatial delay can be determined. Path length differences across the aperture cause phase variation between elements, which must be corrected for optimal beam formation.

The path length difference is given by:

The spatial phase delay, Φ_{spd}, can be expressed mathematically as given in Equation (1).

$$\Phi_{spd} = -k_0 R_i \quad (1)$$

Where Ri is the distance of the feed center from the ith element, and ko is the wave number at the center frequency. A spherical beam is transformed into a collimated beam in the broadside direction when such a distribution is made. Equation (2) below provides the progressive phase shift needed to form this collimated beam.

$$\varphi_{pp} = -k_0 \bar{r_i} \hat{r_0} \quad (2)$$

Here, $\hat{r_0}$ Is the direction of the main beam and $\bar{r_i}$ is the position vector of the ith element. These relationships ensure that a spherical beam from the feed is transformed into a collimated beam. In practice, parallel and closely spaced 'S' curves at different frequencies indicate a wider bandwidth, as phase variation remains consistent across the frequency range.

3.4. S-Curve Analysis for Patch Length Variation

To further optimize the reflectarray unit cell design, multiple Swastik configurations with extended lines were examined by varying the patch length. The reflection phase response of each configuration was analyzed through S-curve measurements, which illustrate the variation of phase shift as a function of patch width for specific frequencies.

Figures 6-8 present the S-curves for patch lengths of 7.2 mm, 7.3 mm, and 7.5 mm, respectively. These curves provide insight into both the achievable phase range and the parallelism of phase variation across the operating frequency band, two critical indicators of bandwidth performance.

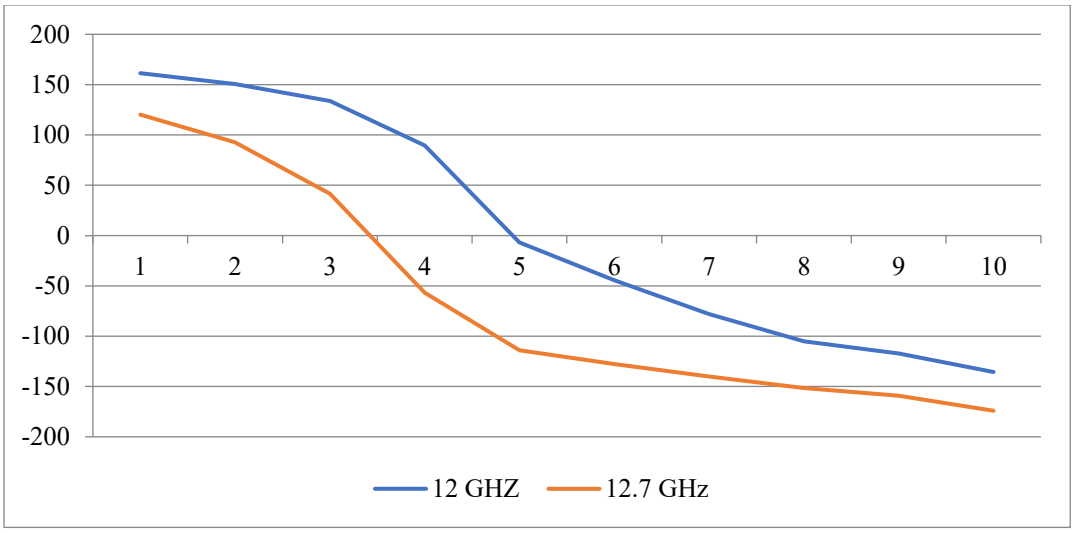

Fig. 6 S Curve for length 7.2 mm

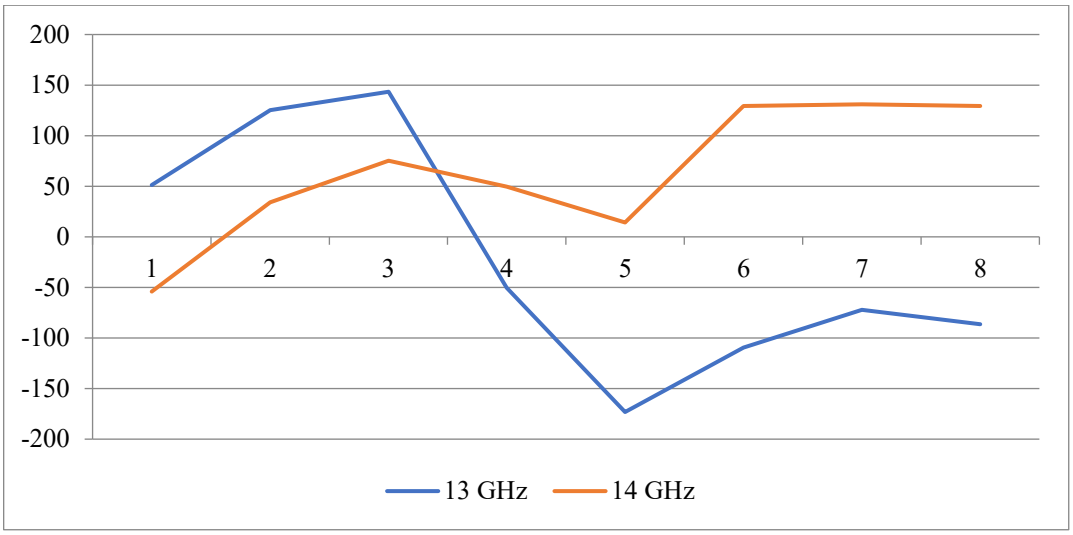

Fig. 7 S Curve for length 7.3 mm

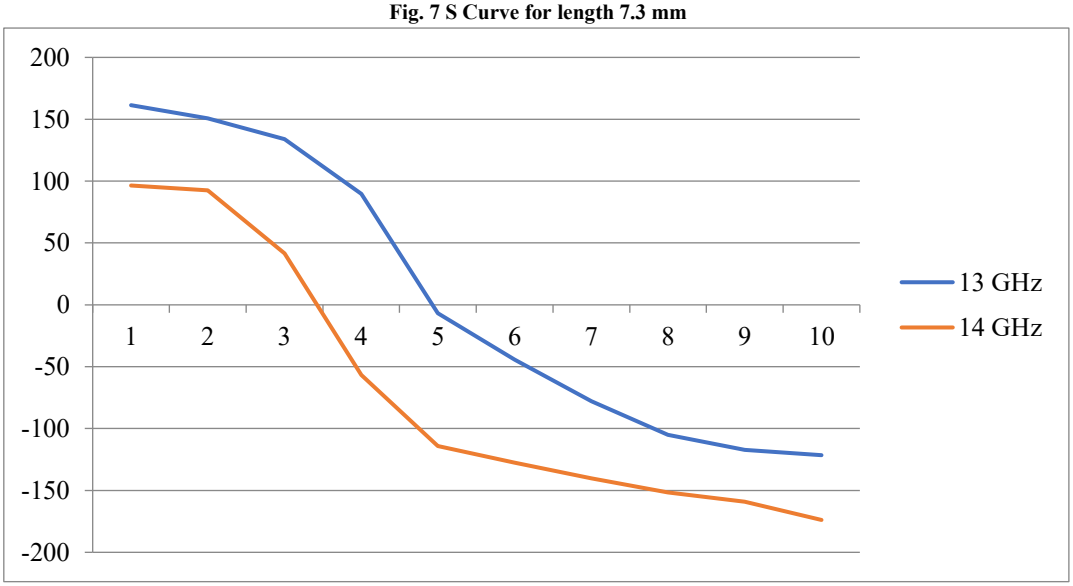

Fig. 8 S Curve for length 7.5 mm

For the 7.2 mm patch length, the phase shift changes from +161.38° to –135.56° at 12 GHz, and from +120.21° to –174.06° at 12.7 GHz, as shown in Figure 6. The parallelism between the curves at these frequencies yields an effective bandwidth of 0.7 GHz. While functional, this configuration provides a smaller usable bandwidth compared to longer patch lengths. Figure 7 shows that at 13 GHz, the phase shift ranges between +172.76° and –136.15° at a length of patch 7.3 mm and between +129.14° and –179.76° at 14 GHz. The better matching of the S-curves at these increased frequencies gives a 1 GHz bandwidth. The phase progression in this length is also smoother, and this can be used to stabilize the steering of the beam. For the 7.5 mm patch length in Figure 8, the phase shift extends from +161.3° to –117.28° at 12 GHz, and from +96.47° to –173.85° at 13 GHz, also providing a 1 GHz bandwidth. This design exhibits greater overall. Phase variation compared to the shorter lengths allows for finer phase and can be used in the applications of aperture variations.

Table 3. Phase Values for Different Patch Lengths

Patch Length	Start Phase	End Phase	Bandwidth
7.2 mm	161.8°	–135.5°	0.7 GHz
7.3 mm	129.1°	–179.76°	1 GHz
7.5 mm	161.3°	–117.2°	1 GHz

The results are summarized in Table 3, which consolidates the start phase, end phase, and bandwidth for each patch length. While both the 7.3 mm and 7.5 mm lengths provide similar bandwidths, the 7.5 mm length offers a broader phase variation range, making it particularly advantageous for high-performance Ku-band reflectarray applications.

The S-curve patterns are due to effective electrical length and coupling changes with patch length. The 7.5 mm version incorporates longer current paths (via the longer lines), thus the resonance frequency shifts, and the phase swing is greater, providing greater phase control than 7.3 mm and 7.2 mm. The difference in bandwidth is proportional to the parallelism of the S-curves in frequency; the more parallel the curves, the wider the usable band (hence ~1 GHz at 7.3/7.5 mm vs. ~0.7 GHz at 7.2 mm). Small simulation-measurement differences are due to fabrication tolerances, fringing fields, connector launches, and substrate variation in εr/tanδ. The comparative analysis confirms that the Swastik geometry with extended lines delivers the most favourable combination of bandwidth, phase tunability, and return loss among all tested designs. Between the two best-performing lengths, 7.3 mm and 7.5 mm, the latter demonstrates a slightly larger phase range, enabling more precise control of aperture phase distribution.

Given its 1 GHz bandwidth, enhanced phase agility, and structural compatibility with fabrication constraints, the As 7.5 mm Swastik design gave robust performance in the range of 12-14GHz band, and is identified as the optimal choice for incorporation into the final reflectarray configuration.

4. Conclusion

The research methodically studied the design and analysis of unit cells to improve reflectarray antenna qualities within the Ku-band (12–14 GHz) for satellite communication, radar, and high-data-rate wireless links. Several figures for the radiating element were investigated, such as rectangular, circular, slotted rectangular (with two and four slots), and the Swastik figure with extended lines. Simulation results demonstrated that patch geometry significantly influences phase tuning range, reflection efficiency, polarization, and angular stability. Full-wave electromagnetic simulations using Floquet ports and master–slave boundary conditions allowed accurate characterization under periodic boundaries, replicating an infinite array. Among the designs investigated, the swastik patch with extended lines provided the best overall performance, combining a wide reflection-phase range (278.5°, approaching 360°), compact footprint (7.5 × 6 mm), large reflection magnitude minima of −26.69 dB and −33.86 dB at 13.8/14.8 GHz, and good polarization stability owing to its symmetric current paths. Its symmetrical design and the many current paths yielded an intricate, adjustable resonance, permitting much more flexibility than traditional and slotted patches. Simulation results were verified by fabrication and experimental validation of the optimized Swastik unit cell, which is a confirmation that it can be used to make practical applications. The small-scale prototype indicates how it is easy to insert into high-density reflectarrays without compromising performance. Finally, this study provides a solid design and analysis framework of reflectarray unit cells and supports the decisive role of radiating element geometry on reflection phase characteristics. Swastik unit cell with long lines appears to be a good candidate for next-generation reflectarrays due to phase agility, simplicity in design, and miniaturization. The findings offer a way forward to reconfigurable, adaptive, and steerable reflectarray systems to support superior satellite communications, new 5G/6G-based infrastructure, and dynamic beam control platforms.

References

[1] D. Berry, R. Malech, and W. Kennedy, "The Reflectarray Antenna," *IEEE Transactions on Antennas and Propagation*, vol. 11, no. 6, pp. 645-651, 1963. [CrossRef] [Google Scholar] [Publisher Link]

[2] Carmen S. Malagisi, "Electronically Scanned Microstrip Antenna Array," *US Patent 4053895A*, pp. 1-7, 1977. [Google Scholar] [Publisher Link]

[3] Thomas Allan Metzler, "*Design and Analysis of a Microstrip Reflectarray*," University of Massachusetts Amherst, Thesis, 1993. [Google Scholar]

[4] D.M. Pozar, and T.A. Metzler, "Analysis of a Reflectarray Antenna Using Microstrip Patches of Variable Size," *Electronics Letters*, vol. 29, no. 8, pp. 657-658, 1993. [CrossRef] [Google Scholar] [Publisher Link]

[5] J. Huang, and R.J. Pogorzelski, "A Ka-Band Microstrip Reflectarray with Elements Having Variable Rotation Angles," *IEEE Transactions on Antennas and Propagation*, vol. 46, no. 5, pp. 650-656, 1998. [CrossRef] [Google Scholar] [Publisher Link]

[6] J.A. Encinar, "Design of Two-Layer Printed Reflectarrays Using Patches of Variable Size," *IEEE Transactions on Antennas and Propagation*, vol. 49, no. 10, pp. 1403-1410, 2001. [CrossRef] [Google Scholar] [Publisher Link]

[7] Arun Bhattacharyya, "Slot-Coupled Patch Reflect Array Element for Enhanced Gain-Band width Performance," *US Patent 6388620B1*, pp. 1-15, 2002. [Google Scholar] [Publisher Link]

[8] M. Bozzi, S. Germani, and L. Perregrini, "Performance Comparison of Different Element Shapes Used in Printed Reflectarrays," *IEEE Antennas and Wireless Propagation Letters*, vol. 2, pp. 219-222, 2003. [CrossRef] [Google Scholar] [Publisher Link]

[9] D.M. Pozar, "Bandwidth of Reflectarrays," *Electronics Letters*, vol. 39, no. 21, pp. 1490-1491, 2003. [CrossRef] [Google Scholar] [Publisher Link]

[10] D.M. Pozar, "Wideband Reflectarrays Using Artificial Impedance Surfaces," *Electronics Letters*, vol. 43, no. 3, pp. 148-149, 2007. [CrossRef] [Google Scholar] [Publisher Link]

[11] Payam Nayeri, Fan Yang, and Atef Z. Elsherbeni, *Bandwidth of Reflectarray Antennas*, Reflectarray Antennas: Theory, Designs, and Applications, pp. 113-145, 2018. [CrossRef] [Google Scholar] [Publisher Link]

[12] Sean Victor Hum, and Julien Perruisseau-Carrier, "Reconfigurable Reflectarrays and Array Lenses for Dynamic Antenna Beam Control: A Review," *IEEE Transactions on Antennas and Propagation*, vol. 62, no. 1, pp. 183-198, 2013. [CrossRef] [Google Scholar] [Publisher Link]

[13] Muhammad Hashim Dahri et al., "A Review of Wideband Reflectarray Antennas for 5G Communication Systems," *IEEE Access*, vol. 5, pp. 17803-17815, 2017. [CrossRef] [Google Scholar] [Publisher Link]

[14] Payam Nayeri, Fan Yang, and Atef Z. Elsherbeni, *Broadband and Multiband Reflectarray Antennas*, Reflectarray Antennas: Theory, Designs, and Applications, pp. 179-225, 2018. [CrossRef] [Google Scholar] [Publisher Link]